

Freeform fabrication of functional aluminium prototypes using powder metallurgy

T. B. SERCOMBE, G. B. SCHAFFER

Department of Mining, Minerals and Materials Engineering, The University of Queensland, St Lucia, 4072, Australia

P. CALVERT

Department of Materials Science and Engineering, The University of Arizona, Tucson, AZ, 85721

E-mail: g.schaffer@minmet.uq.edu.au

Freeform fabrication methods allow the direct formation of parts built layer by layer, under the control of a CAD drawing. Most of these methods form parts in thermoplastic or thermoset polymers, but there would be many applications for freeform fabrication of fully functional metal or ceramic parts. We describe here the freeforming of sinterable aluminium alloys. In addition, the building approach allows different materials to be positioned within a monolithic part for an optimal combination of properties. This is illustrated here with the formation of an aluminium gear with a metal-matrix composite wear surface. © 1999 Kluwer Academic Publishers

1. Introduction

Extrusion freeform fabrication (EFF) is a stereodeposition technique which involves writing a highly loaded ceramic/metal slurry in a 2D pattern on a build platform. The slurry can solidify by a number of mechanisms such as thermal polymerisation, reaction with the atmosphere, or by drying [1]. Successive layer-wise deposition of material builds a 3D part. Post deposition processing is essentially similar to that of powder injection moulded parts and involves removal of the binder and sintering of metal or ceramic powders to high density. Freeform fabrication allows parts to be made directly from a 3D CAD file and therefore lends itself to rapid prototyping.

Parts have been produced by EFF in ceramics [2], as well as thermoplastics [3] and epoxy resin [4, 5] with and without fibre-reinforcement. Multiphase jet solidification, a similar technique developed independently at the Fraunhofer Institute for Applied Materials Research (IFAM), Bremen, Germany, can produce parts from low melting point metals, stainless steel and ceramic powders [6–8].

EFF also has the potential to produce materials and complex geometries that cannot be made in any other way, such as a ball in a box, and functionally graded materials. In addition to rapid prototypes, EFF of components allows a whole new range of products to be made. Functionally graded materials (FGMs) are a typical example. FGMs are a class of material which are deliberately inhomogeneous. The gradients are designed at the microstructural level in order to take advantage of each material type and to develop specific properties and performance requirements. One example is rocket nozzles, where a heat-resistant ceramic surface is graded

to a tough, thermally conductive backing [1]. Selectively reinforced metal matrix composites are another example [1]. Production of such components is facilitated when material can be laid down sequentially, unconstrained by conventional tooling. A series of materials can be deposited in successive planes, or within planes, by selectively adding a reinforcement to desired sections of specific components.

It is a requirement of these techniques that sintering to high density can be effected without compaction. This has not previously been possible with aluminium and its alloys due to the thermodynamic stability of the oxide. At 600 °C, an oxygen partial pressure of $<10^{-50}$ atmospheres [9] or a dew point less than -140 °C [10] is required to reduce the oxide layer. Neither of these are obtainable. Shear during compaction is usually relied upon to disrupt the oxide film sufficiently to allow sintering. Recent work [11] has detailed the role of small levels of Mg on the sintering of Al-alloys. The Mg reacts with the aluminium sesquioxide forming spinel, facilitating disruption of the layer and allowing wetting of sintering liquids. It has also been shown [12] that Sn is an excellent sintering aid for Al and that alloys containing 8% Sn can be sintered to near full density in short times.

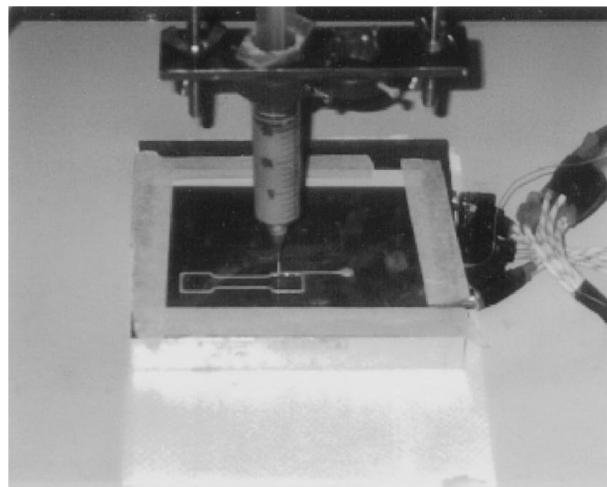
Here we combine extrusion freeform fabrication with the Al-Sn-Mg powder alloys to produce functional aluminium prototypes.

2. Experimental techniques

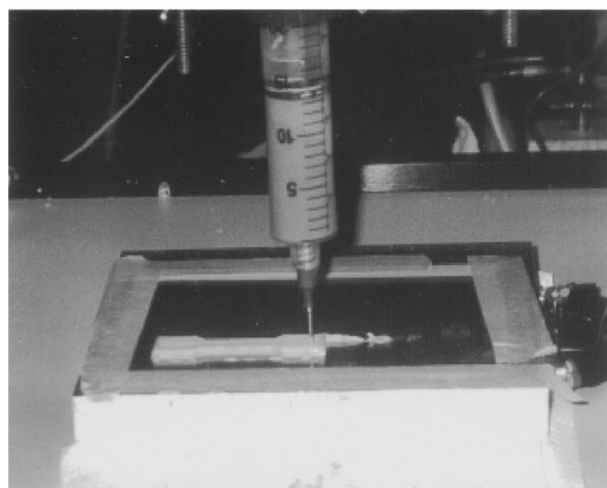
The EFF apparatus for this work comprised an Asymtek (Carlsbad, CA) Fluid Dispenser fitted with a stepper motor-driven syringe, working like a pen plotter. Parts

TABLE I Alloys used for rapid prototyping

		Alloy composition (wt %)			Binder	Binder : powder weight ratio
Sn	Mg	Al ₂ O ₃	Al			
8	3, 5 and 7	0	balance	PVAc	10:13.5	
8	2, 4, 6 and 8	0	balance	PMMA	10:24	
8	6	0, 10, 20, 30 and 40	balance	PMMA	10:24	



(a)



(b)

Figure 1 A tensile specimen being free formed using the EFF technique. (a) Just after the profile of the first layer has been completed and (b) a near complete tensile bar.

were designed in Autocad and the 3D design sectioned into layers, if necessary. Each layer was defined by a perimeter and internal contours, Fig. 1a. Files describing the layers were exported to the Asymtek control system as a series of points.

Alloy compositions and binders are shown in Table I. All compositions are in weight percent. Elemental powders were weighed to an accuracy of 0.01 g and mixed in a rotating mill for 1 h. The Al powder size was $<20 \mu\text{m}$, the Mg and Sn $<45 \mu\text{m}$, and the Al₂O₃ was $22 \mu\text{m}$. All had a purity greater than 99%. Two binders were used: polymethylmethacrylate (PMMA, MW 540,000) and

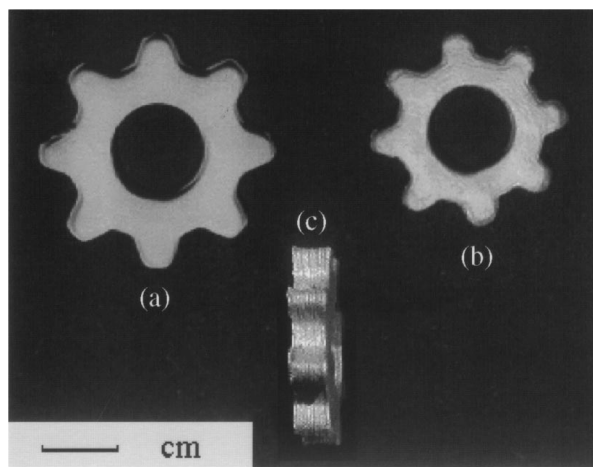


Figure 2 Free formed functionally gradient gears. (a) Green part, (b) sintered and (c) sintered showing layer construction.

polyvinylacetate (PVAc, MW $\sim 100,000$). The polymer was added as a 10% solution in dioxane. Powder/polymer slurries were mixed in a syringe, and left to stand for 15 min to allow removal of trapped gas. Material was extruded through a 0.84 mm (0.033 in.) flat tip needle, using an Oriel (Stratford CT) stepper motor, onto a heated plate at $60 \pm 1^\circ\text{C}$. For successful delivery, a high viscosity PMMA-dioxane solution was needed to suppress preferential extrusion of the liquid phase with a reduced powder concentration. As material is deposited, the dioxane evaporates, leaving a polymer-powder mixture. The apparatus is shown in Fig. 1. A typical part is shown in Fig. 2.

After freeforming, parts were left overnight to allow the dioxane to completely evaporate. Specimens were placed on a bed of alumina and covered with a stainless steel boat. Sintering was performed in a dry nitrogen atmosphere. The cycle consisted of 60 min at 350°C , followed by 30 min at 620°C . The heating rates were approximately 10 and 7°C min^{-1} to the debinding and sintering temperatures, respectively. After sintering, specimens were removed from the furnace and air cooled.

The sintered density was determined by Archimedes method as per Metal Powder Industries Standard 42, "Determination of Sintered Density of Compacted or Sintered Metal Powder Products", with the exception that alcohol was used instead of water. Specimens for metallographic investigation were vacuum impregnated in epoxy resin, ground to 1200 grit, polished with Brasso and Silvo (domestic polishing compounds; Reckitts Household Products, Sydney, Australia) and finished with $0.05 \mu\text{m}$ silica. Specimens were sputter coated with either gold or platinum and were examined in a Jeol 820 SEM. Tensile specimens were tested in an Instron 1026 screw machine with a cross head speed of 0.6 mm min^{-1} . Strain was measured using an extensometer with a 12.5 mm gauge length and 20% full scale. Thermogravimetric analysis (TGA) of green specimens was performed on a Perkin Elmer TGA7 under high purity N₂. Samples weighing 15–17 mg were heated at $100^\circ\text{C min}^{-1}$ to 250, 300 or 350°C and held for up to 60 min.

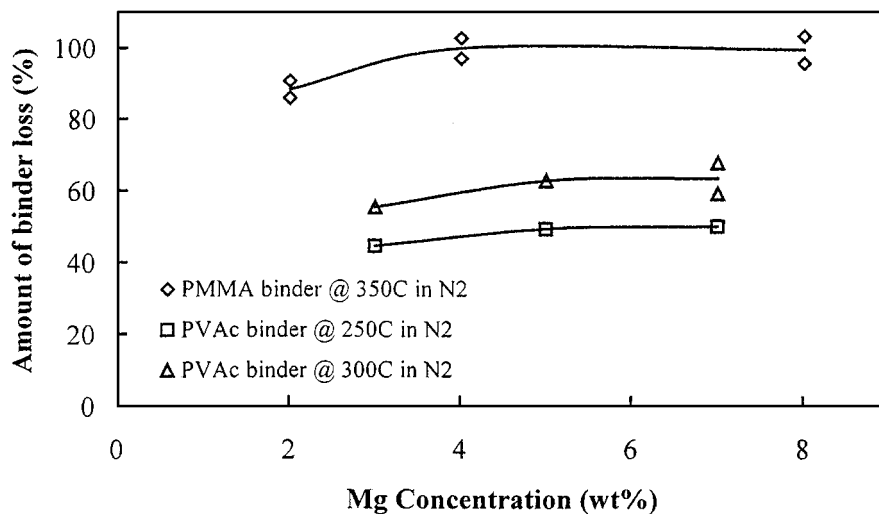


Figure 3 Amount of resin lost during debinding as a function of Mg content in the specimens containing PVAc at 250 and 300 °C and PMMA at 350 °C. For the PMMA, almost all the resin is lost, whereas ~50% of the PVAc is lost at 250 °C and 60% at 300 °C. The data points show individual specimens.

3. Results and discussion

Isothermal TGA was performed at 250 and 300 °C for Al-8Sn-3, 5 and 7Mg alloys with 7.4% PVAc as the binder and at 350 °C for Al-8Sn-2, 4, and 8Mg alloys with 4.2% PMMA binder. Fig. 3 shows the weight loss as a percentage of the total binder. A value of 100% would be recorded when all of the binder is removed. For the PMMA binder, there is almost complete resin removal. However, only about 50% of the PVAc is removed. The thermal decomposition of the PVAc in N₂ results in the production of acetic acid and other volatile organic compounds, with some carbon residue. This residue remains in the debinded part and interferes with sintering. There may also be some reaction between the acetic acid and the Al, Mg and Sn powders. PMMA, however, decomposes principally by unzipping, with the loss of monomer units as vapour. Since the green density of these parts is low, the vapour is easily removed from the part. As a result, there is little residue remaining after debinding. It appears that PMMA is a superior binder to PVAc and PMMA was therefore used as the binder in all subsequent work.

The sintered density as a function of Mg content and typical microstructures are shown in Figs 4 and 5, re-

spectively. Approximately 4% Mg is required to produce peak density. In pressed and sintered parts, the oxide break-up due to shear during compaction is aided by the reaction of Mg with the oxide [11]. Since there is no compaction in freeformed parts, oxide break up must occur solely via reaction with the Mg. The peak in density occurs at a much higher Mg content (4% vs. 0.15%) in freeformed parts than in pressed specimens. This difference may be explained by the extremely low green density of the freeformed parts and lack of neck formation in the green body. In pressed specimens, the oxide on the Al particles not immediately in contact with the Mg is exposed via diffusion of Mg through the bulk. Since necks form during compaction and the diffusivity of Mg in Al is very high [13], Mg may diffuse through many powder particles. The same is not possible for unpressed parts. Hence, significantly more than the theoretical amount of Mg is required to reduce all of the oxide. The excess Mg will remain in solution in the Al, and contribute to solid solution strengthening.

Al and Sn are mutually insoluble in the solid phase, but there is a high solubility of Al in liquid Sn once the temperature exceeds about 580 °C. Additionally, no intermetallics form and their liquids are miscible. Since

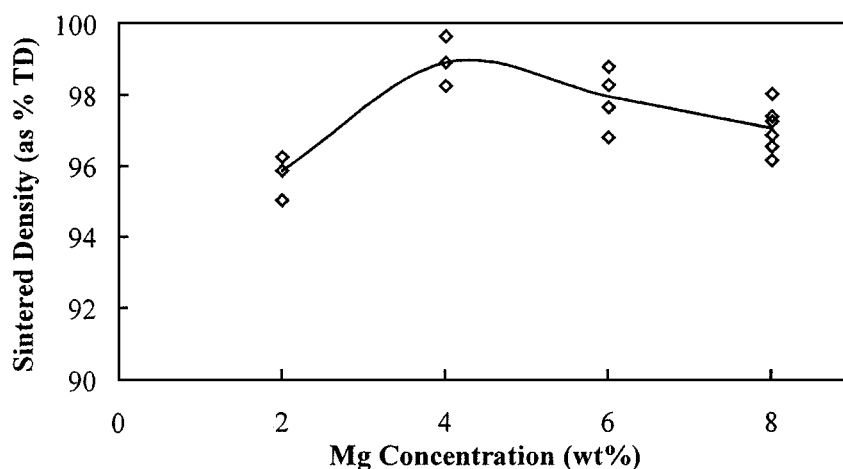
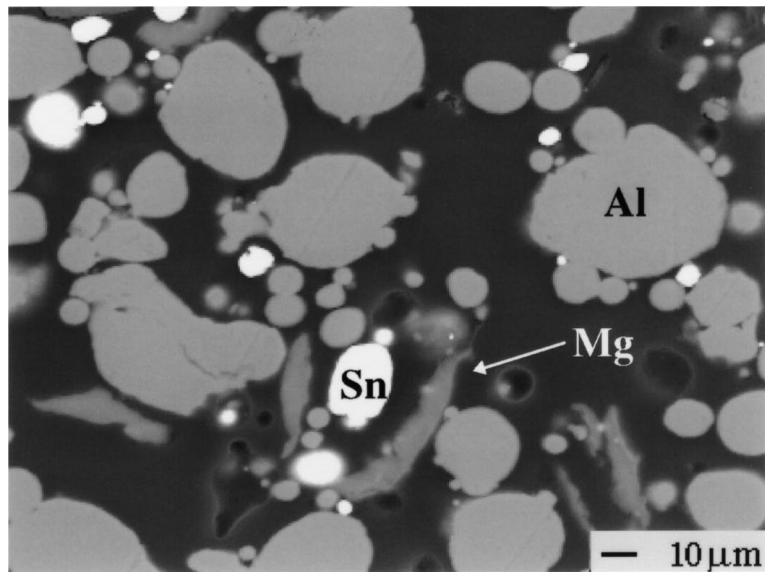
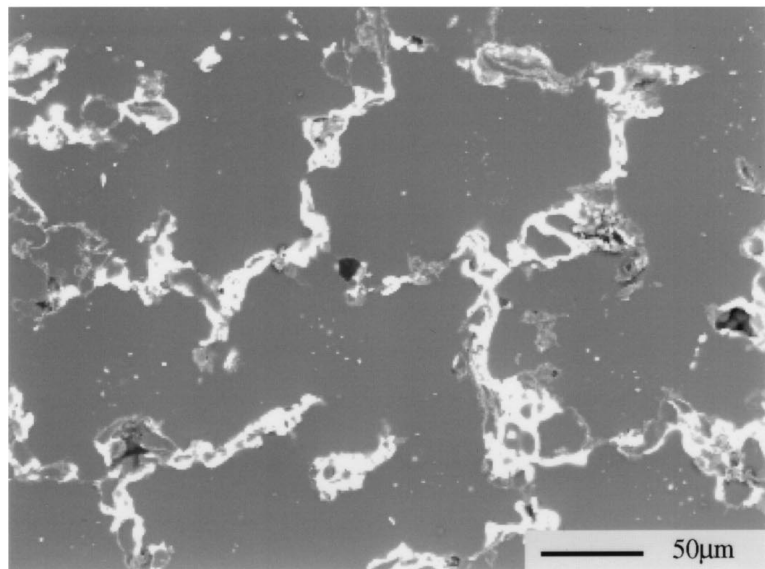


Figure 4 The role of Mg on the sintered density of free formed Al-8Sn tensile bars. Data points show individual specimens, the line joins median values. There is a peak in density at 4% Mg.



(a)



(b)

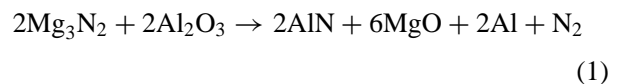
Figure 5 Backscattered scanning electron micrographs of an Al-8Sn-6Mg alloy (a) as fabricated and (b) as sintered.

Sn is virtually insoluble in Al, the liquid phase will persist throughout the entire sintering cycle. As a consequence, near full density can be achieved from green densities of $\sim 50\%$ (Fig. 4).

Specimens need to be covered for sintering to be most effective. The covers consisted of thin gauge stainless steel sheet, bent into the form of a boat. These covers were inverted and placed over the specimens prior to sintering. Although they did not provide a sealed environment, they shielded the specimens from direct gas flow. Sintering under argon was ineffective regardless of whether the specimens were covered or not. In a N_2 atmosphere only the covered specimens sintered. This suggests that there is some interaction between the sample and the atmosphere, which facilitates sintering.

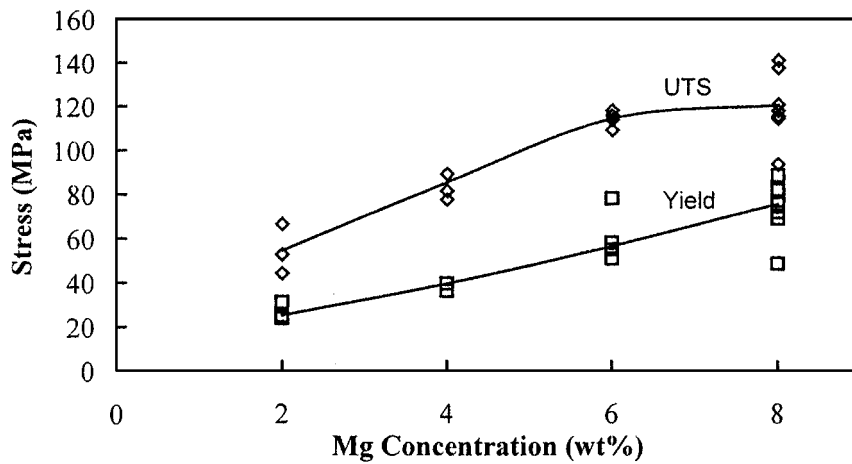
It has been reported in the patent literature [14] that formation of Mg_3N_2 occurs when Mg is vapourised into a nitrogen atmosphere. Reduction of the oxide was

then thought to occur by reaction of the Mg_3N_2 with the oxide:

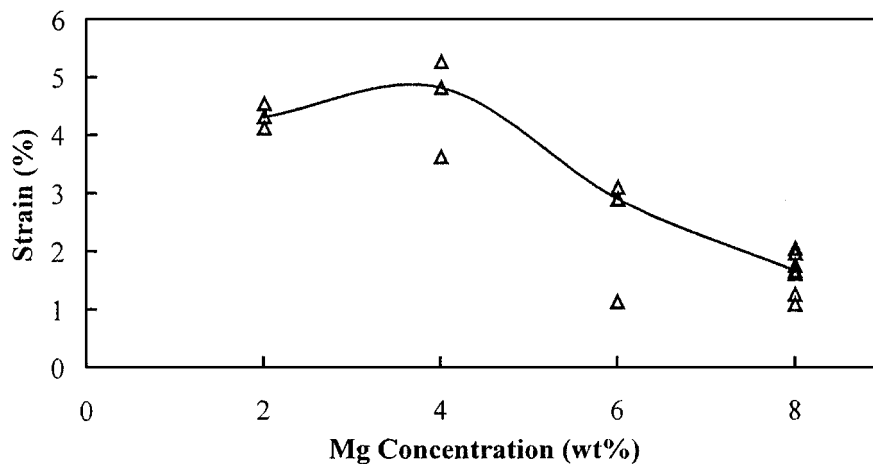


The reaction between Mg and N_2 at sintering temperatures only occurs in the vapour state [14]. Therefore, it is a requirement that Mg vapour is present during sintering. Mg loss due to vapourisation has been detected above $200^\circ C$ [15] and increases with temperature. It is possible that Mg_3N_2 forms during sintering and covering the specimens traps the nitride in the vicinity of the part, where it may react with the oxide layer according to Equation 1. Without the covers, the nitride is blown downstream of the parts and is therefore ineffective.

In the absence of a major strengthening mechanism, the tensile strengths (Fig. 6a) are comparable



(a)



(b)

Figure 6 As sintered tensile properties for freeformed tensile bars containing 8% Sn and various Mg levels. (a) Yield and UTS and (b) strain to failure. Data points show individual specimens, the line joins median values. There is a peak in ductility at 4% Mg, the same amount required to produce maximum density.

to pressed-and-sintered Al-Sn-Mg compacts [12]. The use of pre-alloyed powders may be necessary to increase strength and ductility. The low ductility (Fig. 6b) in comparison to pressed and sintered parts of similar compositions [12] may be due to the relatively high density of oxides at the original particle boundaries, because of the comparatively fine Al powder used here. The test bars also warped slightly with the upper, last deposited layer concave. This distortion, with a deflection of about 1 mm over 5.5 cm, corresponds to a strain of ~2% in the surface. This distortion originates during forming, not sintering and may be due to un-even settling of each layer which, in turn, may be an effect of non-uniform evaporation of the solvent from different sections of the specimen. Prevention of this distortion may be possible via the use of thin layers or having longer intervals between the deposition of layers.

A series of specimens containing Al-8Sn-6Mg and up to 40 wt % alumina were produced and sintered. The sintered density of these alloys is shown in Fig. 7. A loading of 10% has no effect on the sintering response. As the alumina content is increased above this level, the amount of shrinkage decreases until, at 40 wt % addition, little densification occurs. A similar response occurs in pressed and sintered composites [16–19]. The

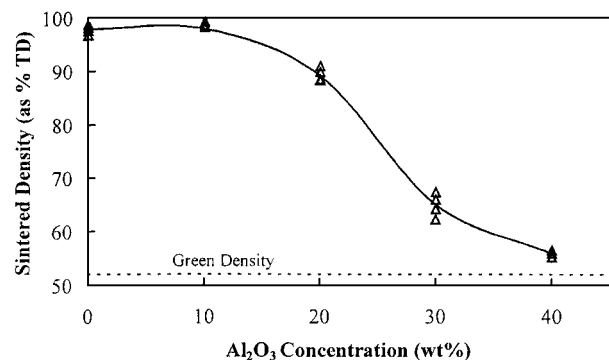
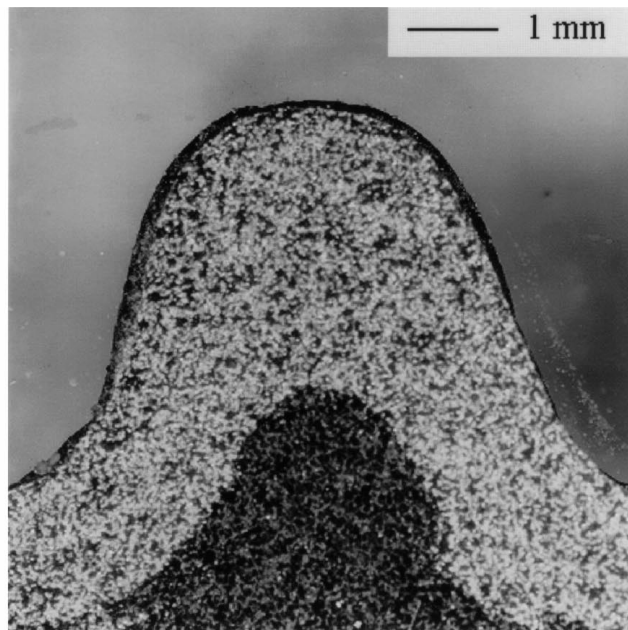
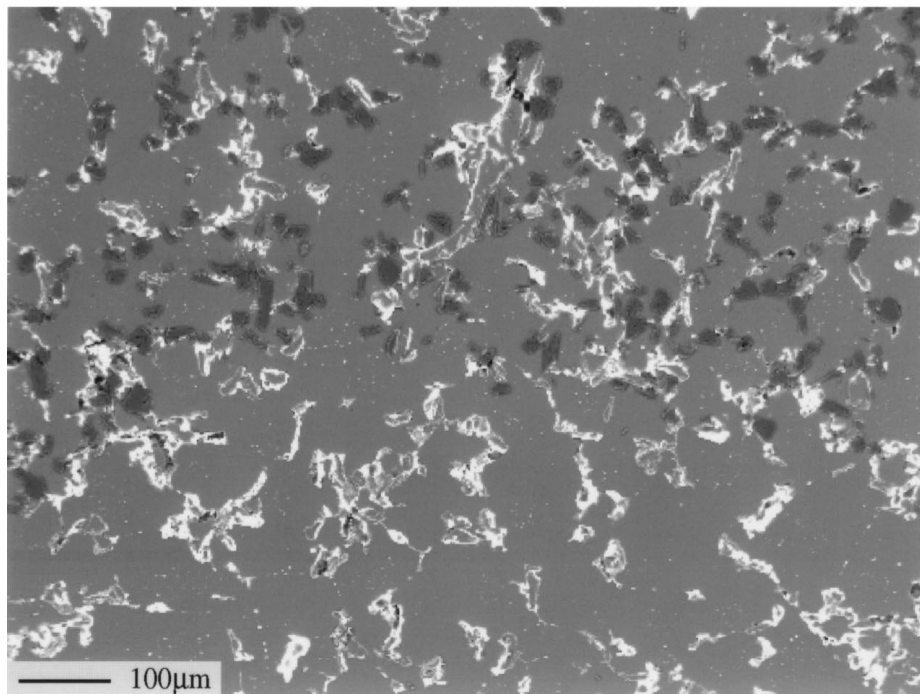


Figure 7 The effect of Al₂O₃ on the sintering of free formed Al-8Sn-6Mg alloys. The addition of 10 wt % Al₂O₃ has no effect on the sintering of these alloys. For additions greater than this amount, there is a steady decrease in the sintered density and almost no shrinkage occurs at 40%. Data points show individual specimens, the line joins median values.

ability to manufacture functionally graded parts is one of the advantages of this approach. Functionally graded material gears were freeformed and sintered. The outside of the gear was made from Al-8Sn-6Mg-10Al₂O₃; while the bulk contained an alumina free alloy. The microstructure is shown in Fig. 8. The contact surface contains a hard ceramic component which will improve



(a)



(b)

Figure 8 Microstructures of an FGM gear. (a) Optical micrograph of a gear tooth with alumina containing alloy on the outside of the gear. (b) Backscattered scanning electron image of the interface between the two regions. There is perfect bonding between the layers.

wear resistance and the inside of the gear, which has no such wear requirement, does not. Fig. 8a shows a single gear tooth, while the interface between the two alloys is shown in Fig. 8b.

4. Conclusions

Unlike conventional powder metallurgy where metal powders are pressed to dense preforms, freeform fabrication methods produce green bodies at about 60 vol % metal plus a polymer binder. In the absence of interparticle bridges, which generally form during mechanical

compaction, this low packing density retards sintering. We have shown for the first time that aluminium alloys, composites and functionally graded materials can be produced and sintered to near full density using extrusion freeform fabrication.

The polymer binder must be selected to not interfere with post-deposition processing. PMMA, which decomposes by unzipping, is preferred to PVAc which decomposes under nitrogen to form acetic acid. We describe an easily sinterable alloy, which does not require mechanical compaction and can be pressureless sintered. The metal component consists of aluminium

powder, which is mixed with magnesium powder to reduce surface oxides and with tin powder to provide an ideal sintering system. A typical alloy composition is Al-8Sn-4Mg. Alumina additions of up to 10 wt % can be incorporated without decreasing the sintered density.

Freeform fabrication of metals offers a way of making intricate parts that cannot be machined, of making structures with graded compositions and of incorporating internal closed porosity to reduce weight.

Acknowledgements

In Australia, this work was funded by the Department of Industry, Science and Tourism under the Bilateral Science and Technology Program and by the Australian Research Council. We would like to thank the National Science Foundation for support for the US part of this work under grant DMI 94 20356 and The Queensland University of Technology for support of PDC during sabbatical leave.

References

1. P. CALVERT and R. CROCKETT, *Chemistry of Materials* **9** (1997) 650.
2. K. STUFFLE *et al.*, in Proceedings of the Solid Freeform Fabrication Symposium, edited by H. L. Marcus *et al.* (Austin, Texas, 1993) p. 60.
3. R. S. CROCKETT *et al.*, in Proceedings of the Solid Freeform Fabrication Symposium, edited by H. L. Marcus *et al.* (Austin, Texas, 1995) p. 17.
4. P. CALVERT *et al.*, *Chemistry of Materials* **8** (1996) 1298.
5. J. LOMBARDI *et al.*, *Polymer Preprints* **37** (1996) 221.
6. M. GREUL *et al.*, *Computers in Industry* **28** (1995) 23.
7. M. GREUL, *Materials Technology* **11** (1996) 131.
8. M. GREUL *et al.*, *Metal Powder Report* **52** (1997) 24.
9. L. S. DARKEN and R. W. GURRY, in "Physical Chemistry of Metals" (McGraw Hill, New York, 1953).
10. C. LALL, *Int. J. Powder Metall.* **27** (1991) 315.
11. R. N. LUMLEY *et al.*, *Metallurgical Transactions A* **30A** (1999) 457.
12. T. B. SERCOMBE and G. B. SCHAFFER, in Advances in Powder Metallurgy and Particulate Materials: Proceedings of the 1997 Conference on Powder Metallurgy and Particulate Material, 1997.
13. H. MEHER, in "Landolt Bornstein Numerical Data and Functional Relationships in Science and Technology," Vol. III/26 (Springer-Verlag, Berlin, 1991), p. 151.
14. Y. NAKAO *et al.*, US Patent no. 5,525,292 (1996).
15. I. KOVACS *et al.*, *Materials Science and Engineering* **21** (1975) 169.
16. H. DANNINGER, *Metal Powder Report* (UK) **48** (1993) 46.
17. A. K. JHA *et al.*, *Powder Metallurgy* **32** (1989) 209.
18. G. H. BORHANI *et al.*, *ibid.* **36** (1993) 67.
19. R. Q. GUO *et al.*, *J. of Mater. Sci.* **32** (1997) 3971.

Received 17 February 1998
and accepted 17 February 1999